Hydrogen bond studies in substituted *N*-(2-hydroxyphenyl)--2-[(4-methylbenzenesulfonyl)amino]acetamides

Liliana Aguilar-Castro,[a] Margarita Tlahuextl,[a] Luis H. Mendoza-Huizar,[a] Antonio R. Tapia-Benavides,[a]* and Hugo Tlahuext[b]

[a]Centro de Investigaciones Químicas, Universidad A. del Estado de Hidalgo, Carretera Pachuca-Tulancingo Km 4.5. U. Universitaria. C.P. 42184 Mineral de la Reforma, Hidalgo, México

[b]Centro de Investigaciones Químicas, Universidad A. del Estado de Morelos, Av. Universidad 1001 Col., Chamilpa, CP 62100, Cuernavaca Morelos, México

E-mail: tapiab@uaeh.reduaeh.mx

Dedicated to Professor Rosalinda Contreras on the occasion of her 60th birthday

Abstract

Six substituted *N*-(2-hydroxyphenyl)-2-[(4-methylbenzensulfonyl)amino]acetamides **7**-**12** have been synthesized from 2-amino-3-nitrophenol, 2-amino-4-nitrophenol, 2-amino-5-nitrophenol, 2-amino-4-chlorophenol, 2-amino-4-*tert*-butylphenol, 2-amino-4-chloro-5-nitrophenol, and the [(4-methylbenzenesulfonyl)amino]acetyl chloride derivative of [(4-methylbenzenesulfonyl)amino]acetic acid. These compounds have been characterized by FAB mass spectrometry, IR, and NMR (^{1}H, ^{13}C, ^{15}N) spectroscopy. Variable temperature NMR experiments on compounds **7**-**12** gave evidence for the formation of intra- and intermolecular hydrogen-bonds in solution. The molecular structure of **7** and **12** was determined by X-ray crystallography. The electronic behavior of the intramolecular hydrogen-bonds in these compounds was established by NBO studies.

Keywords: Phenolamides, ^{1}H, ^{13}C, ^{15}N NMR, X-ray, DFT, NBO, hydrogen-bond

Introduction

Non-covalent interactions have fundamental roles in supramolecular chemistry, drug design, protein folding, crystal engineering and other areas of molecular science[1]. Hydrogen-bond interactions are principal forces which determine the recognition phenomena, self-assembly processes and the structure of a great variety of chemical and biological systems[2]. A hydrogen-bond, X-H•••Y, is an interaction wherein a hydrogen atom (which is covalently united to X) is

attracted to another atom (Y). It has been recognized since early times that this attraction always increases with the electronegativity of X and Y[3], and the electrostatic nature of all hydrogen-bonds is accepted without doubt. Hydrogen-bonds are electrostatic interactions but the proportion of electrostatic character can vary[4] and the presence of these interactions can be explained on the basis of two stabilizing mechanisms:

1) If X and Y are electronegative atoms, the hyperconjugative interaction (which is often called covalent component or charge transfer component) is present due to the partial transfer of alone pair of electrons of Y to the antibonding orbital of X-H [n(Y)→σ*(X-H)]. The hyperconjugative interaction increases the electronic population of the σ*(X-H) orbital and produce the elongation of the X-H bond[5]. When the hyperconjugative phenomenon is dominant, this interaction is denominated as a "proper hydrogen-bond"[6-7].

2) If X is not an electronegative atom, but this atom is able to undergo changes in hybridization and polarization, the presence of Y reduces the length of X-H and increases the s-character of the X-H bond[6-8]. In this case, the X-H•••Y interaction is called an "improper hydrogen-bond"[6-7].

Both factors are present in all types of H-bonds, but the prevalence of improper interactions is likely to be observed when the charge transference n(Y) → σ* (X-H) is weak[7]. C-H bonds are able to form hydrogen-bond interactions when they are under the action of substituent groups that cause them to become good σ-acceptors or make them to have significant rehybridization[7].

On the other hand, *N*-(2-hydroxyphenyl)-2-[(4-methylbenzenesulfonyl)amino]acetamides (or *N*-(*p*-toluenesulfonyl)-glycine-2-phenolamides) are useful intermediates in the synthesis of heterocyclic compounds with potential biological activity[9-12]. The molecular structure of these compounds is interesting because there are intramolecular O•••H•••N and C-H•••O interactions that constrain the geometry of the amide in the *E,Z* conformation (**A** in Scheme 1)[13]. However, it is the *Z,Z* conformer (**B** in Scheme 1) that is required to produce the cyclization reaction and the presence of these intramolecular hydrogen interactions avoids benzoxazole formation. We have found that *tert*-butyl groups in the benzene ring restrict the presence of intramolecular C6-H6•••O2 hydrogen-bonds[13]. The amide group in these compounds is not coplanar with the aromatic ring and electronic conjugation between these groups is unlikely. Thus, the presence of electron donor groups in the benzene ring restrict the participation of N-H in hydrogen-bond interactions and thus the *Z,Z* conformation (**B** in Scheme 1) is favored in these amides[13].

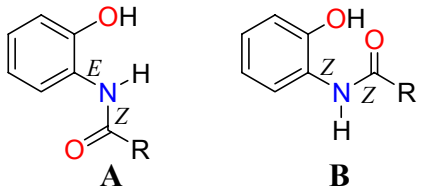

Scheme 1. Conformation of amide group in 2-phenolamides

Thus, the presence of electron withdrawing groups in the benzene ring of *N*-(2-hydroxyphenyl)-2-[(4-methylbenzenesulfonyl)amino]acetamides could modify the σ-acceptor

capacity of the C6-H6 bond or it could increase the electronegativity of C6 and promote the formation of C6-H6•••O2 hydrogen-bonds. In order to analyze the electronic factors involved during the processes mentioned above, in this paper we synthesized six substituted *N*-(2-hydroxyphenyl)-2-[(4-methybenzenelsulfonyl)amino]acetamides **7-12** (Scheme 2). These amides were characterized by NMR, X-ray crystallography and NBO studies.

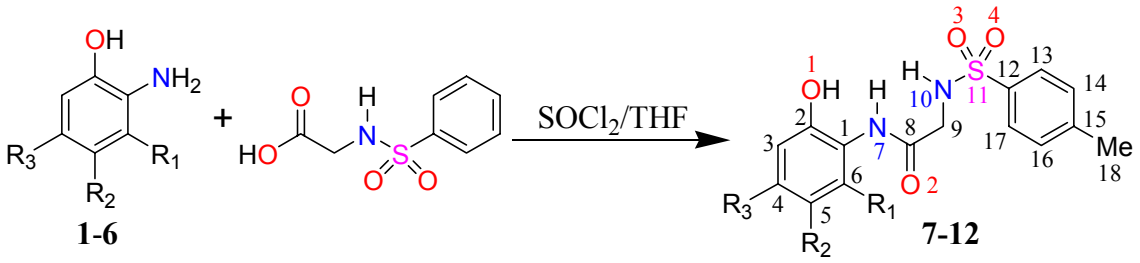

1 and **7** $R_1 = NO_2$; $R_2 = H$; $R_3 = H$
2 and **8** $R_1 = H$; $R_2 = NO_2$; $R_3 = H$
3 and **9** $R_1 = H$; $R_2 = H$; $R_3 = NO_2$
4 and **10** $R_1 = H$; $R_2 = Cl$; $R_3 = H$
5 and **11** $R_1 = H$; $R_2 = Bu^t$; $R_3 = H$
6 and **12** $R_1 = H$; $R_2 = Cl$; $R_3 = NO_2$

Scheme 2. Synthesis of substituted *N*-(2-hydroxyphenyl)-2-[(4-methylbenzenesulfonyl)amino] acetamides **7-12.**

Results and Discussion

N-(2-Hydroxyphenyl)-2-[(4-methylbenzenesulfonyl)amino]acetamides **7-12** were obtained in yields above 75% by a established protocol[12-13]. The molecular structure of amides **7-12** was unequivocally established by FAB mass spectrometry, IR and NMR (^{1}H, ^{13}C, ^{15}N) spectroscopy. In order to assign all the NMR signals, heteronuclear correlation experiments (HETCOR) were carried out. The conformational studies in solution of **7-12** were performed by multinuclear magnetic resonance and variable temperature experiments.

NMR studies in solution

In the ^{13}C NMR spectra of amides **8-12** the chemical shifts of C6 show dependence with respect to the substitution of the benzene ring (Table 1). The C6 nuclei appear at different frequencies showing the influence of the electronic behaviour of the substituent group and their relative position in the ring. Therefore, the magnitude of the electronic density present at C6 is different in amides **8-12**. On the other hand, C8 in **7-12** has similar chemical shifts compared with those amides where the carbonyl group is conjugated with the aromatic ring[13]. This fact demonstrates

that the substitution of the benzene ring in **7-12** did not inhibit the electronic conjugation between the aromatic ring and the carbonyl group.

Table 1. ^{13}C NMR (δ in ppm) of **7-12** in DMSO-d6

	C1	C2	C3	C4	C5	C6	C8	C9	C12	C13 C17	C14 C16	C15	C18
7	126.5	152.5	114.7	120.1	117.7	146.1	166.8	45.3	137.4	126.6	129.6	142.8	21.0
8	126.1	153.4	114.6	120.6	139.1	115.4	167.3	46.0	137.1	126.7	129.6	143.0	20.9
9	132.8	146.6	109.1	143.1	115.3	118.8	167.6	46.1	137.0	126.5	129.7	142.6	21.0
10	127.0	145.8	116.0	123.5	122.1	119.7	166.8	45.9	137.0	126.7	129.6	142.9	20.9
11	125.2	144.8	114.7	117.8	141.2	121.0	166.4	45.9	137.0	126.7	129.6	142.9	21.0
12	131.7	145.8	111.6	141.1	115.9	120.7	167.8	46.0	137.1	126.7	129.6	142.9	20.9

^{15}N NMR chemical shifts of nitrogen N7 in amides **7-12** (Table 2) have the normal values for 2-phenolamides with intramolecular hydrogen bonding[13-14]. Moreover, these chemical shifts are similar to amides where the amide group is delocalized into the aromatic ring[15]. The coupling constants ^{1}J(N-H) = 90-93 Hz for N7 suggest that the hydrogen atom is strongly bonded to nitrogen and also indicate a trigonal planar geometry at the N7 atoms[16]. However, the ^{15}N NMR chemical shifts of N10 appeared at higher frequencies [Δδ = 17-27 ppm] with respect to N7 and show that these nitrogen atoms tend to have pyramidal geometries.

Table 2. ^{1}H TV-NMR (Δδ/ΔT in ppm K^{-1}) and δ ^{15}N of **7-12** in DMSO-d6

	-Δδ/ΔT N-H7	$-\Delta\delta/\Delta T$ N-H10	$-\Delta\delta/\Delta T$ C-H5	$\delta\,^{15}N$ N7-H	$\delta\,^{15}N$ N10-H
7	0.0013	0.0046		-267	-289
8	0.0012	0.0035	0.00057	-257	-278
9	0.0019	0.0037	0.00054	-255	-278
10	0.0034	0.0016	0.00046	-259	-276
11	0.0011	0.0026	0.00011	-259	-286
12	0.0021	0.0039	0.00002	-256	-276

It has been accepted that the ^{1}H NMR chemical shifts dependence on the temperature**,** ($\Delta\delta/\Delta T$) is a diagnostic tool to determine if the hydrogen atoms have intra-intermolecular or solvent interactions[17-18]. Thus, in DMSO-d6 solution, where the values ($\Delta\delta/\Delta T$) are lower than 3 x 10^{-3} ppm/K, intramolecular hydrogen bonding is present**.** On the other hand, values higher than 4 x 10^{-3} ppm/K are attributed to solvated N-H groups. We studied the nature of hydrogen-bond interactions by variable temperature ^{1}H NMR ($\Delta\delta/\Delta T$) in compounds **7-12** (Table 2). The chemical shifts of H7 signals in compounds **7-9, 11** and **12** showed a small variation with the temperature ($\Delta\delta/\Delta T$ from -1.1 to -2.1 x 10^{-3} ppm/K); therefore, we conclude that H7 in these amides has intramolecular hydrogen-bonds. The different electronic nature of the groups on the

benzene ring affects the mobility of H7. For example, amide **10** has a chlorine atom on C5, and the electronegative behaviour of the Cl atom reduces the electronic density of the phenyl oxygen. Thus, in **10** no intramolecular H-bond of H7 ($\Delta\delta/\Delta T$ = -3.4 x 10^{-3} ppm/K) is present. On the other hand, in amide **11** the electron donor activity of the *tert*-butyl group increases the electronic density on the phenyl oxygen and consequently H7 ($\Delta\delta/\Delta T$ = -1.1 x 10^{-3} ppm/K) has a strong intramolecular O1•••H7 hydrogen-bond. The dependence of the chemical shift with respect to temperature of H10 shows that this atom presents intermolecular interactions in amides **7-9** and **12**. However, in compounds **10-11** the $\Delta\delta/\Delta T$ values indicate that H10 has intramolecular interactions. Thus, it is probable the presence of intramolecular interactions O2•••H10 in **10-11**. Therefore, these compounds have different conformations in solution than amides **7-9**.

Table 3. ^{1}H NMR (δ in ppm) of **7-12** in DMSO-d6

	O-H1	C-H3	C-H4	C-H5	C-H6	N-H7	C-H8	N-H10	C-H13 C-H17	C-H14 C-H16	C-H18
7	10.62	7.30	7.22	7.22		9.74	3.68	8.01	7.72	7.37	2.35
8	12.00	7.15	7.93		8.90	9.45	3.75	8.30	7.75	7.39	2.36
9	11.29	7.72		7.72	8.26	9.50	3.74	8.28	7.72	7.37	2.34
10	10.48	6.94	6.94		7.95	9.26	3.66	8.27	7.73	7.37	2.35
11[a]	9.75	6.80	6.93		7.93	9.20	3.61	8.25	7.73	7.39	2.36
12	11.66	7.66			8.26	9.60	3.76	8.26	7.70	7.36	2.34

[a] 1.21 $C(CH_3)_3$

The chemical shift for H7 reflects the force of the hydrogen-bonds in these compounds. It is known that the presence of strong hydrogen-bond makes significant changes in the chemical shifts of the hydrogen signals toward high frequencies[19-20]. Thus, the signals of H7 in **10-11** are displaced towards minor frequencies (Δδ = 2.10-1.48 ppm) than the corresponding signals in **7-9** and **12** (Table 3). This fact confirms that, in DMSO-d6 solution, **7-9, 12** do not have the same hydrogen bonding arrangement than **10** and **11.** Chemical shifts for H6 in **8-12** showed that this atom has intramolecular interactions with O2[14]. Thereby, in compounds **10-11** the intramolecular interactions H6•••O2•••H10 are present, where O2 acts a pivot of a pseudobicyclic system.

X-Ray crystallography studies

The recrystallization processes of compounds **7** and **12** yielded crystals that were suitable for the X-ray crystallographic studies. Perspective views of molecular geometries of these compounds are shown in Figure 1. The most relevant crystallographic data and the hydrogen-bond interactions for amides **7** and **12** have been summarized in Table 4. The X-ray crystallography study corroborates the influence of the substituent groups about the conformation of amides in solid state. Amide **7** has the *Z,Z* conformation where the hydroxyl and carbonyl group are in the

same side [C8-N7-C1-C2 = -45.0(4)º], whereas the amide **12** has the *E,Z* conformation with the hydroxyl and carbonyl groups on different sides [C8-N7-C1-C6 = -19.1(9)º].

Table 4. Crystal data for compounds **7** and **12**

Crystal data	**7**	**12**
Formula	$C_{15}H_{15}N_3O_6S$	$C_{15}H_{14}ClN_3O_6S$
MW (g mol^{-1})	365.36	399.80
Space group	P2(1)/n	Cc
	Cell Parameters	
a (Å)	16.427(7)	31.657(2)
b (Å)	5.240(2)	7.3658(5)
c (Å)	19.632(8)	7.7285(6)
α (º)	90.00	90.00
β (º)	97.976(9)	101.674(2)
γ (º)	90.00	90.00
V (Å^3)	1673.4(11)	1764.9(2)
Z	4	4
μ(mm^{-1})	0.231	0.373
ρ (g cm^{-3})	1.450	1.505
	Data Collection	
θ limits (Å)	1.74 < θ < 25.0º	1.31 < θ < 29.04º
hkl limits	-19,19; -6,6; -23,17	-42,27; -9,10; -10,10
No. Collected refl.	9471	7230
No. Ind refl. (R_{int})	2945 (0.1031)	3619 (0.0772)
	Refinement	
R	0.0467	0.0513
Rw	0.1049	0.1206
No. Of variables	287	256
GOF	0.976	1.001
$\Delta\rho_{min}$ (e Å^{-3})	-0.321	-0.316
$\Delta\rho_{max}$ (e Å^{-3})	0.225	0.416

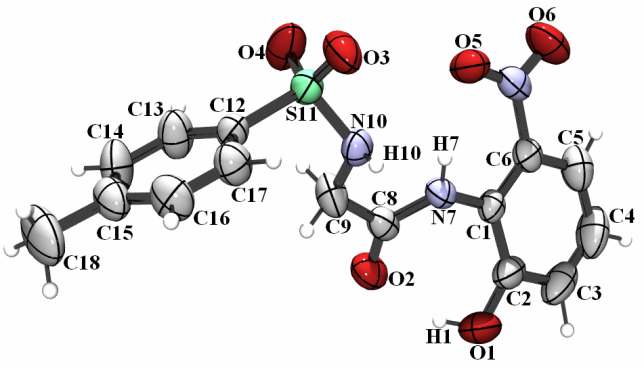

Compound 7

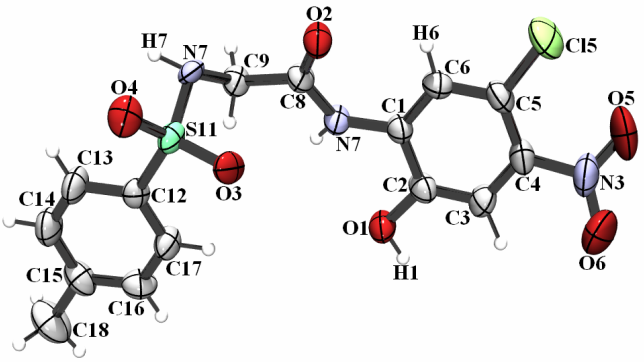

Compound 12

Figure 1. X-Ray molecular structure of **7** and **12.**

Table 5. Hydrogen-bond and contact geometry of compounds **7** and **12**

Compound	D—H•••A	D-H	H•••A	D•••A	<(D—H•••A)
7	N7-H7···O6^{i}	0.81(3)	2.55(3)	3.148(4)	131(2)
	N10-H10···O4^{ii}	0.74(3)	2.22(3)	2.921(4)	157(3)
	O1-H1···O2	0.87(4)	1.784(5)	2.587(3)	152(4)
	N7-H7···O5	0.81(2)	2.111(3)	2.620(3)	121(2)
	N7-H7···N10	0.81(2)	2.339(3)	2.726(3)	110(2)
12	O1-H1···O2^{iii}	0.91(7)	1.75(7)	2.656(5)	179(8)
	N10-H10···O4^{iv}	0.88(7)	2.14(7)	2.911(6)	146(5)
	N7-H7···O3^{v}	0.87(5)	2.34(5)	3.199(6)	173(4)
	N7- H7···O1	0.87(5)	2.41(5)	2.614(6)	94(4)
	C6-H6···O2	0.87(6)	2.42(6)	2.861(8)	112(5)

Symmetry codes: (i) -x+3/2, y-½, -z+½; (ii) x, y-1, z; (iii) x, y+1, z; (iv) x, -y-1, z+1/2; (v) x, -y, z+1/2.

In amide **7** where there is a NO_2 group at C6 the N7-H7•••O5 interaction is formed (Table 5). Moreover, the phenolyc hydrogen H1 has a strong interaction with O2 [O1-H1•••O2 = 1.784(5)

Å] (**A** in Figure 2). The nitrogen atoms N7 and N10 are *syn* [the torsional angle N10-C9-C8-N7 is -13.8(4)º] and the intramolecular hydrogen bonding N7-H7•••N10 is possible (Table 4). The length between N7 and N10 in the amide **7** is 2.726(3) Å, which is below the sum of the van der Waals radii of nitrogen atoms (r_{RVD} = 3.1 Å) corroborates the intramolecular H-bond N7-H7•••N10. The molecular structure of **7** is further stabilized by the N7-H7•••O6 intermolecular interaction (**A** in Figure 2) and the presence of N10-H10•••O4 hydrogen-bond chains running along the b axis (**B** in Figure 2).

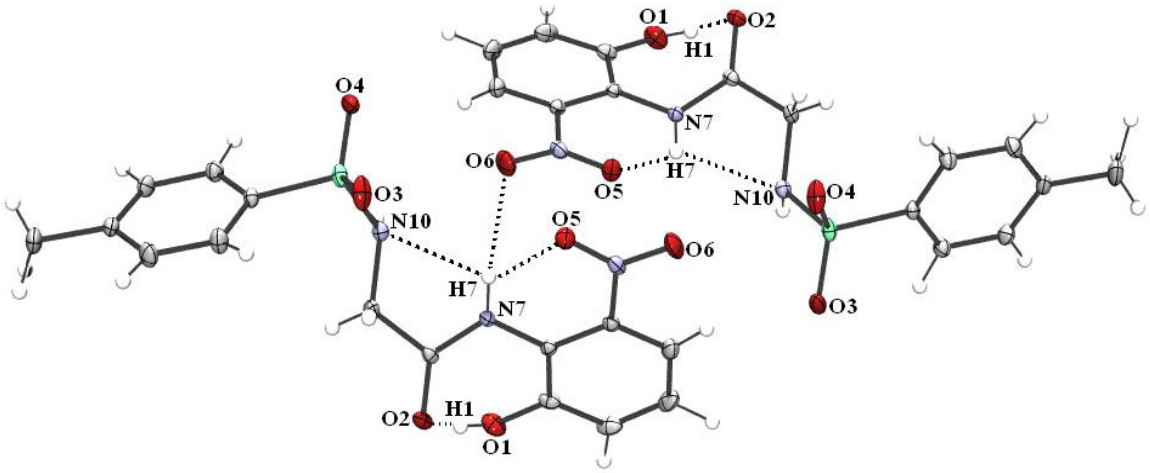

A

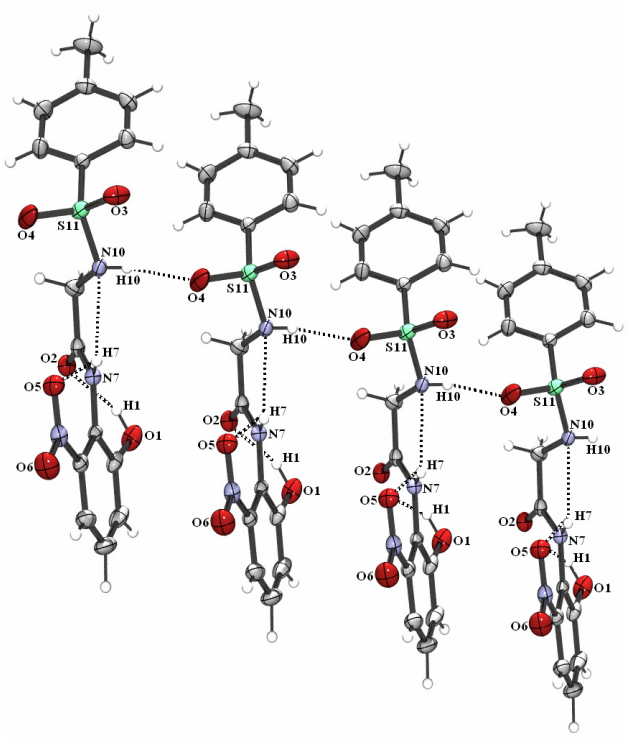

B

Figure 2. Hydrogen-bond interactions in amide **7.**

The bond distance between C6 and O2 in **12** is 2.861(8) Å, which is below the sum of the van der Waals radii of carbon and oxygen (r_{RVD} = 3.10 Å), shows the possible presence on intramolecular hydrogen-bonds C6-H6•••O2 (Figure 3)[15]. On the other hand, despite of the *syn* a arrangement of N7 and N10 in **12** [N10-C9-C8-N7 is 142.6(5)º] and the distance between O2•••N10 is 2.842(6) Å, the N10-H10 bond does not point towards O2 and therefore there is no O2•••H10-N10 hydrogen-bond in compound **12**. However, the bond distance between H7 and O3 (2.34(5) Å) shows the presence of the intramolecular hydrogen-bond N7-H7•••O3. Finally, the packing is stabilized too by intermolecular O1-H1•••O2 hydrogen-bond chains running along the *b* axis.

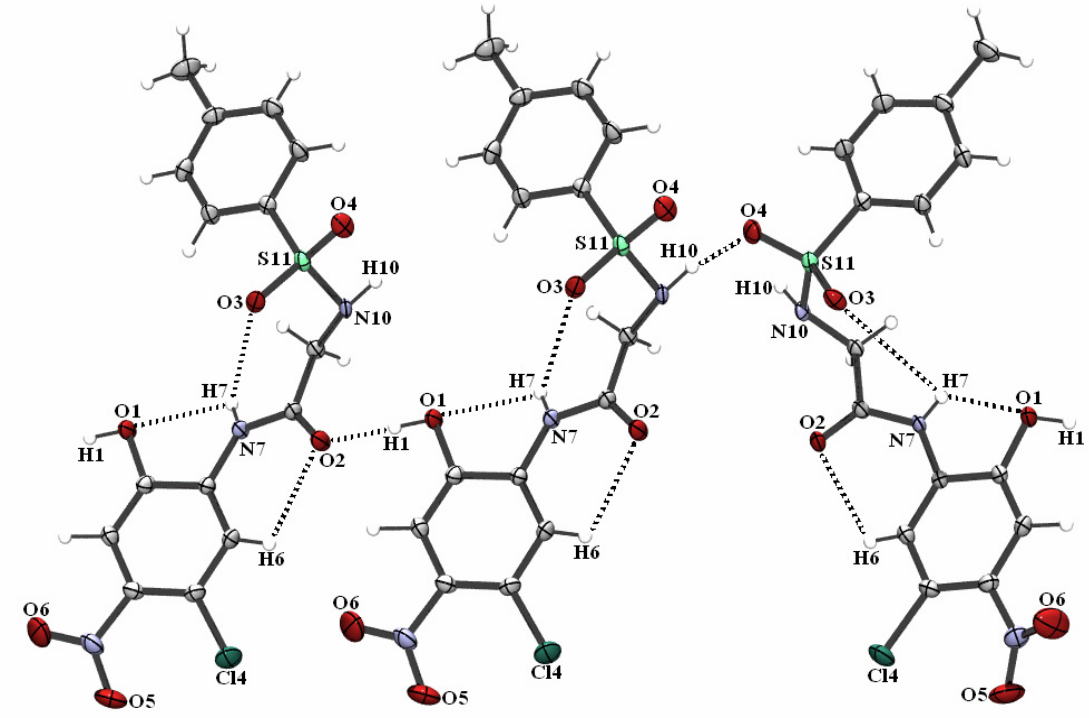

Figure 3. Hydrogen-bond interactions in amide **12.**

Theoretical studies

It has been accepted that Density Functional Theory (DFT) calculations provide an accurate description of the electronic and structural properties of amides[22-26]. In this work, we have performed full geometry optimizations with no symmetry restrictions of **7**-**12** at ab initio B3LYP exchange-correlation density functional with a 6-311G++(d,p) basis set[27-29]. Once the lowest energy species were obtained, vibrational frequencies were computed to make sure that the global minima on the potential energy surfaces were indeed obtained. From theoretical calculations, the geometries of **7**-**12** obtained showed that these amides have the C_1 point group (Figure 4). The optimized geometrical parameters (lengths and bond angles) of **7** and **12** (Table 6) were compared with the X-ray experimental results and were found to be similar (the determination coefficient R^2 for bond lengths is 0.9841 for **7** and 0.9880 for **12**) and (R^2 for bond

angles is 0.9726 for **7** and 0.9762 for **12**). It is interesting to observe that except for N10-S11 bond, the average error between experimental measurements in bond lengths is lesser than 2% compared to theoretical calculations. However, the error involved in the N10-S11 bond are 4.7% and 5.6 % for structure **7** and **12**, respectively. Thus, it is necessary to mention that optimized structures **7** and **12** were obtained at gas phase, since the experimental structure is in solution. It is possible to observe that the bond length more affected is precisely the N10-S11. Thus from calculation it is possible to deduce that the N10-S11 bonding is lightly compressed by a solution effect. In accordance with X-ray diffraction, calculations showed that N7 in compounds **7**-**12** have trigonal geometries and are in agreement with the chemical shifts observed in ^{15}N NMR. However, N10 atoms tend to have pyramidal geometries with the *t*etra*h*edral *c*haracter (THC) from 40.13 to 75.6 % [30].

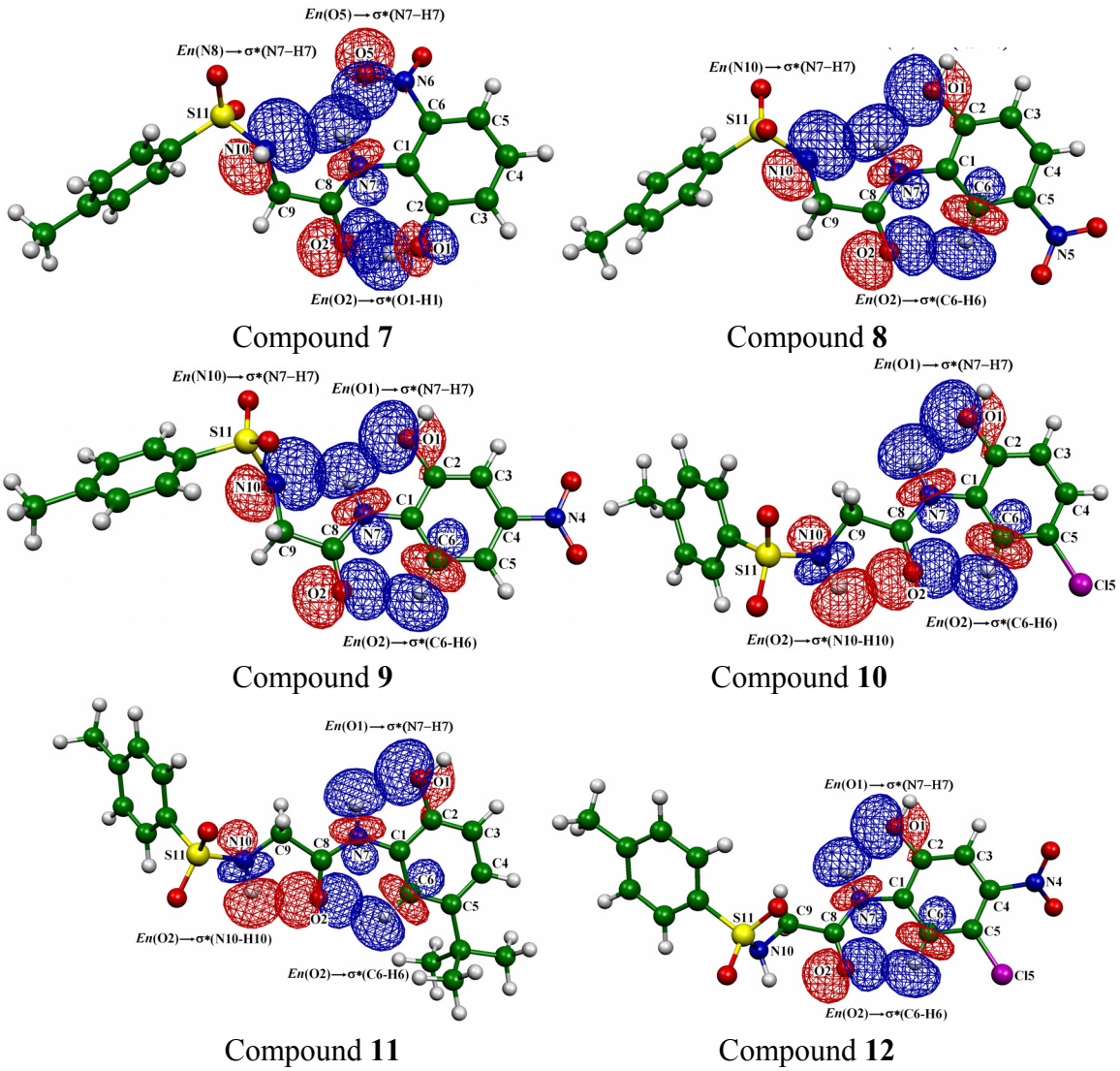

Compound **7** Compound **8**

Compound **9** Compound **10**

Compound **11** Compound **12**

Figure 4. Optimized structures (**7**-**12**) at B3LYP 6-311++G(d,p) level and *En*→σ* hydrogen interactions.[31]

Table 6. Theoretical and experimental lengths and bond angles for **7** and **12** molecules in the ground state

	Structure **7**		Structure **12**	
Parameters	X-ray	B3LYP/ 6-311++G(d,p)	X-ray	B3LYP/ 6-311++G(d,p)
Bond lengths				
O1-C2	1.360(4)	1.348	1.366(7)	1.370
C2-C3	1.392(5)	1.399	1.367(8)	1.378
C1-C6	1.407(3)	1.415	1.372(8)	1.395
C1-C2	1.406(4)	1.415	1.406(7)	1.411
C1-N7	1.406(3)	1.414	1.424(7)	1.398
N7-C8	1.340(3)	1.356	1.349(6)	1.373
C8-O2	1.229 (3)	1.230	1.212(6)	1.216
C9-N10	1.447(4)	1.458	1.471(7)	1.459
N10-S11	1.622(2)	1.699	1.616(4)	1.701
S11-C12	1.773(2)	1.799	1.764(6)	1.797
Bond angle				
N10-S11-C12	108.0(1)	106.7	110.0(2)	102.0
O1-C2-C1	122.6(3)	123.2	115.4(5)	116.0
N7-C8-O2	124.4(3)	125.5	124.2(5)	124.7
S11-N10-C9	118.6(2)	119.9	116.8(4)	116.5
Dihedral angle				
N10-C9-C8-N7	-13.8(4)	-19.0	142.6(5)	-147.105
C8-N7-C1-C6	138.3(3)	143.2	-19.1(9)	3.335
O2-C8-N7-C1	5.0(4)	4.6	0.4(9)	2.875
O2-C8-C9-N10	166.5(3)	162.0	-38.4(8)	36.635
O1-C2-C1-N7	-1.0(4)	-0.7	0.9(7)	0.301

Natural Bond Orbital (NBO) analysis showed that the sigma bond σ(N7-H7) gets a mayor charge transference (hyperconjugative interaction) in amides **7-9** than that occurring in **10-12** (Figure 4)[7]. Although, in compound **7** the stabilization energy *E* from the interaction of lone pair of electrons of O5 toward σ*(N7-H7) bond is found to be large [*En*(O5)→σ*(N7-H7) = 9.47 kcal mol^{-1}], for compounds **8-12** the stabilization energy *E* from the alone pair electrons of O1 toward σ*(N7-H7) bond is short and similar in all cases (Table 7). However, N7-H7 bond in amides **7-9** had an additional charge transference from the N10 toward σ*(N7-H7) bond. This fact is reflected in the differences of polarization coefficients between N7 and H7 that are more significant in **7-9** than in **10-12**. Additionally, the population of the antibonding σ*(N7-H7) is bigger in **7-9** (Table 8). These results are in accordance with the ^{1}H NMR of **7-12**. The correlation of the chemical shift of H7 with respect to the sum of stabilization energies *E* from

O5 (for **7**), O1 (for **8-12**) and N10 (for **7-9**) towards the σ*(N7-H7) bond**,** showed dependence of the chemical shift and the stabilization energy (Figure 4). Thus, whereas the stabilization energy increases with the number of H-bonds of the N7-H7 moiety, the NMR signal of H7 is shifted toward high frequencies.

Table 7. NBO stabilization energy *En*→σ* in kcal mol^{-1} of intramolecular hydrogen bonding for amides **7-12**

Compound	O2→H1-O1	O2→H6-C6	O1→H7-N7	O5→H7-N7	N10→H7-N7	O2→H10-N10
7	20.02			9.47	2.37	
8		1.78	1.19		2.37	
9		1.65	1.27		2.81	
10		1.61	1.16			1.28
11		1.89	1.09			2.60
12		1.76	1.16			

The experimental data of **8-12** shows the possible presence of the C6-H6•••O2 hydrogen interaction where the ^{1}H NMR of H6 is shifted toward higher frequencies[32]. NBO studies show low charge transference of O2 towards the antibonding σ*(C6-H6) (Table 7). It is known that when hyperconjugation in X-H•••Y systems is weak and the molecular structure should allow significant rehybridization of the X-H bond, the improper H-bonding is possible[6-7]. Thus, changes in the hybridization of C are indeed of non classical hydrogen interaction. The quantum calculations show signs of the rehybridization of C6-H6 bond in amides **8-12**: 1) The C6-H6 bond distance is 0.078-0.024 Å shorter than the rest of the C-H aromatic bonds in **8-12.** 2) The C6-H6 bond has a substantial major *p*-character (from 28.4 to 30.9 %). 3) The charge of H6 is considerably greater than the rest of the C-H aromatic bonds. These results are in agreement with the ^{13}C NMR spectra of **8-12,** the correlation of the chemical shift of C6 with respect to its hybridization shows an exponential dependence (Figure 5). Therefore, the *p*-character increase of C6 shifts their NMR signals towards higher frequencies.

Table 8. Calculated natural hybrids (NHOs), polarization coefficients for σ_{N-H} bonds and population of the antibonding σ*(N-H) orbital of intramolecular hydrogen bonding in amides **7-12**

Compound	σ(N7-H7)	σ*(N7-H7)	σ(N10-H10)	σ*(N10-H10)
7	$0.8614sp^{2.51}+0.5079s$	0.04059	$0.8384sp^{2.65}+0.5450s$	0.01551
8	$0.8524sp^{2.60}+0.5229s$	0.02397	$0.8381sp^{2.69}+0.5456s$	0.01551
9	$0.8535sp^{2.61}+0.5211s$	0.02585	$0.8396sp^{2.58}+0.5433s$	0.01519
10	$0.8439sp^{2.75}+0.5364s$	0.01714	$0.8490sp^{2.48}+0.5284s$	0.02101
11	$0.8434sp^{2.77}+0.5373s$	0.01700	$0.8503sp^{2.49}+0.5264s$	0.02414
12	$0.8459sp^{2.74}+0.5348s$	0.01750	$0.8439sp^{2.71}+0.5366$	0.01626

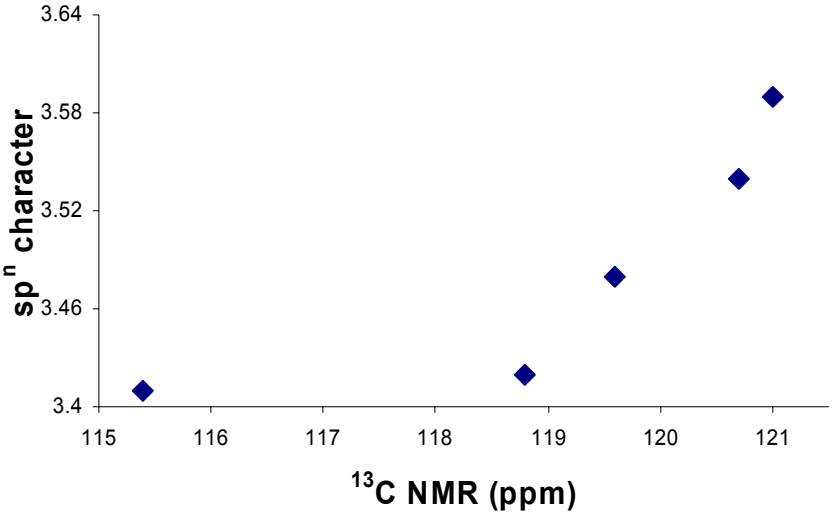

Figure 5. Correlation of sp^n hybridization with δC6 in the ^{13}C NMR spectra in compounds **8-12.**

In conclusion, NMR, crystallographic and DFT theoretical quantum studies have shown that the presence of substituent groups in the aromatic ring modify the force of the intramolecular interactions of the amide N-H hydrogen atoms. Thus, experimental and theoretical methods show that while N7-H7 present classical interactions, the interaction of C6-H6 with O2 are non-classical. The stabilization energy shows that charge transference *En*(O2) → σ*(C6-H6) is more important than *En*(O1) → σ*(N7-H7). Thus, the hyperconjugative and rehybridization events are more important in the C6-H6•••O2 interaction than in N7-H7•••O1. Therefore, it is possible to conclude that the preference of the 2-phenolamides **8-12** for the *E,Z* conformation is due to presence of C6-H6•••O2 interactions.

Experimental Section

General Procedures. All solvents were freshly distilled and dried before use according to established procedures. Melting points were measured on a Mel-Temp II apparatus and are uncorrected. The IR spectra were recorded on a Perkin-Elmer System 200 FT-IR spectrophotometer. Elemental analyses were determined on a Perkin-Elmer Series II CHNS/O analyzer 2400 instrument.

NMR spectra were obtained on a JEOL GXS-400 MHz spectrometer in DMSO-d6 solution. Chemical shifts (ppm) are relative to electronic frequencies $(CH_3)_4Si$ for ^1H and ^{13}C and CH_3NO_2 for ^{15}N NMR. Variable temperature experiments were carried out in DMSO-d6 with a temperature controller to keep the temperature constant within 0.2 ºC. The temperature was varied from 298.15 to 418.15 K. Each spectrum was obtained with 32 scans. ^{15}N NMR spectra

were recorded at 40.51 MHz using a multinuclear 5 mm probe. The DEPT without decoupling pulse sequence was used to detect the ^{15}N signal. The average $^{1}J(^{15}N\text{-}^{1}H)$ value was 89.5 Hz. A spectral width of 32 768 Hz with a digital resolution of 0.99 Hz was used; the pulse delay was 2 s with an acquisition time of 1.35 s.

X-ray data were collected on a Bruker Smart 6000 diffractometer with a CCD area detector with graphite-monochromated Mo-K_α radiation. The measured intensities were reduced to F^2 without absorption correction with the program SAINT-NT[33]. Structure solution, refinement and data output were carried out with the SHELXTL-NT program package[34]. The non-hydrogen atoms were refined anisotropically. All H atoms in compound **7** were located in a difference Fourier map and refined isotropically. In compound **12** with, the exception of H6, H3, N- and O- bound hydrogen atoms, the H atoms were considered with a riding model under restriction of ideal symmetry at the corresponding carbon atoms. Figures were created with Ortep3[35].

Crystallographic data (excluding structure factors) have been deposited with the Cambridge Crystallographic Data Centre as CCDC 650995 and 650996. Copies of the data can be obtained free of charge on application to: The Director, CCDC, 12 Union Road, Cambridge, CB2 IEZ, UK (fax: +44-1223-336-033; e-mail: deposit@ccdc.cam..ac.uk or www.ccdc.cam.ac.uk).

We employed a cluster Beowulf with 14 processors of 3.0 GHZ each one, with 1GB of RAM for all quantum calculations. These calculations were performed with Gaussian 98 ver. A.11[36], Q-chem 3.0[37] packages and visualized with the GaussView V. 3.0,[38] and Molekel 4.3[31] packages. Geometries were fully optimized at the B3LYP/6-311++G(d,p) level of the density functional theory. A set of vibrational frequencies of these compounds were calculated with this level of theory and then scaled by 0.9614. Additionally, NBO 3.0 was used to characterize the intramolecular interactions at B3LYP/6-311++G(d,p) level[39].

***N*-(2-Hydroxy-6-nitrophenyl)-2-[(4-methylbenzenesulfonyl)amino]acetamide (7).** The procedure described below is representative for the synthesis of compounds **7-12**. A solution of *N*-[(4-methylbenzenesulfonyl)amino]acetic acid 100 mg (0.43 mmol) in $SOCl_2$ (1 cm^3) was stirred at 20° for 1 h. The excess of $SOCl_2$ was removed under vacuum and the [(4-methylsulfonyl)amino]acetyl chloride obtained was immediately dissolved in a mixture of 2-amino-3-nitrophenol (66.26 mg, mmol) and THF (25 cm^3). The mixture was stirred for 30 min and the THF removed under vacuum. HPLC on Zorbax ODW C-18 semipreparative column with acetonitrile-water (70:30) as the eluent yielded **7** (110 mg, 70%). Mp 218-219 °C. IR ν_{max} (HATR)/cm^{-1}: 3603 ν(OH), 3359, 3275, 1536, 1240 ν(NH-CO), 1681 ν(C=O), 1329, 1167 ν(SO_2). Found: C, 50.5; H, 4.4; $C_{15}H_{15}N_3O_6S$ $0.2CH_3CN$ requires C, 50.6; H, 4.3. m/z (EI, 70 eV) 365(M^+), 347(M^+-H_2O), 319(365-NO_2), 184(M^+-$C_7H_5N_2O_4$), 181(M^+-$C_8H_{10}NO_2S$), 155(M^+-$C_8H_8N_3O_4$), 154(M^+-$C_9H_9NO_3S$).

***N*-(2-Hydroxy-5-nitrophenyl)-2-[4-methylbenzenesulfonyl)amino]acetamide (8).** *N*-[(4-methylbenzenesulfonyl)amino]acetic acid (100 mg, 0.43 mmol), was treated with $SOCl_2$ (1 cm^3), 2-amino-4-nitrophenol (66.26 mg, 0.43 mmol). The amide was purified by HPLC (70:30 ratio of acetonitrile-water) to yield **8** (110 mg, 70%). Mp 258-260°C. IR ν_{max} (HATR)/cm^{-1}: 3282 ν

(OH), 1536, 1502 ν(NH-CO), 1664 ν(C=O), 1330, 1156 ν(SO_2). Found: C, 48.9; H, 4.2; $C_{15}H_{15}N_3O_6S$ $0.2H_2O$ requires C 48.8; H 4.2. m/z (EI, 70 eV) 365(M^+), 210 (M^+-$C_7H_7O_2S$), 184(M^+-$C_7H_5N_2O_4$), 181(M^+-$C_8H_{10}NO_2S$), 155(M^+-$C_8H_8N_3O_4$), 154(M^+-$C_9H_9NO_3S$).

***N*-(2-Hydroxy-4-nitrophenyl)-2-[(4-methylbenzenesulfonyl)amino]acetamide (9).** *N*-[(4-methylbenzenesulfonyl)amino]acetic acid (100 mg, 0.43 mmol), was treated with $SOCl_2$ (1 cm^3), 2-amino-5-nitrophenol (66.26 mg, 0.43 mmol). The amide was purified by HPLC (70:30 ratio of acetonitrile-water) to yield **9** (97.5 mg, 62 %). Mp 228-229°C. IR ν_{max} (HATR)/cm^{-1}: 3447 ν (OH), 1592, 1560 ν(NH-CO), 1670 ν(C=O), 1320, 1155 ν(SO_2). Found: C, 48.9; H, 4.2; $C_{15}H_{15}N_3O_6S$ $0.15H_2O$ requires C 49.1; H 4.3. m/z (EI, 70 eV) no M^+, 256(M^+-C_7H_9O), 181(M^+-$C_8H_{10}NO_2S$), 91(M^+-$C_8H_8N_3O_6S$).

***N*-(5-Chloro-2-hydroxyphenyl)-2-[(4-methylbenzenesulfonyl)amino]acetamide (10).** *N*-[(4-methylbenzenesulfonyl)amino]acetic acid (100 mg, 0.43 mmol), was treated with $SOCl_2$ (1 cm^3), 2-amino-4-chlorophenol (61.5 mg, 0.43 mmol). The amide was purified by HPLC (70:30 ratio of acetonitrile-water) to yield **10** (94.4 mg, 62 %). Mp 217-219°C. IR ν_{max} (HATR)/cm^{-1}: 3361 ν (OH), 1595, 1550 ν(NH-CO), 1667 ν(C=O), 1344, 1156 ν(SO_2). Found: C, 47.7; H, 4.2; $C_{15}H_{15}ClN_2O_4S$ $1.1H_2O$ requires C, 48.1; H, 4.6. m/z (EI, 70 eV) 354(M^+), 337(M^+-H_2O), 246(337-$C_7H_7O_2S$), 184(M^+-$C_7H_8NO_2S$), 170(M^+-$C_8H_{10}NO_2S$), 91(M^+-$C_8H_8N_2O_4S$).

***N*-(5-*tert*-Butyl-2-hydroxyphenyl)-2-[(4-methylbenzenesulfonyl)amino]acetamide (11).** *N*-[(4-methylbenzenesulfonyl)amino]acetic acid (100 mg, 0.43 mmol), was treated with $SOCl_2$ (1cm^3), 2-amino-4-*tert*-butylphenol (70.95 mg, 0.43 mmol). The amide was purified by HPLC (70:30 ratio of acetonitrile-water) to yield **11** (116.41 mg, 72 %). Mp 193-195 °C. IR ν_{max} (HATR)/cm^{-1}: 3320 ν(OH), 1597, 1542 ν(NH-CO), 1674 ν(C=O), 1327, 1155 ν(SO_2). Found: C, 59.6; H, 6.2; $C_{19}H_{24}N_2O_4S$ $0.35H_2O$ requires C, 59.6; H, 6.5 m/z (EI, 70 eV) no M^+, 283(M^+-C_7H_7), 280(M^+-CH_5NO_3S), 184(M^+-$C_{11}H_{14}NO_2$), 150(M^+-$C_9H_{11}N_2O_3S$).

***N*-(5-Chloro-3-hydroxy-4-nitrophenyl)-2-[(4-methylbenzenesulfonyl)amino]acetamide (12).** *N*-[(4-methylbenzenesulfonyl)amino]acetic acid (100 mg, 0.43 mmol), was treated with $SOCl_2$ (1cm^3), 2-amino-4-chloro-5-nitrophenol (81.1 mg, 0.43 mmol). The amide was purified by HPLC (70:30 ratio of acetonitrile-water) to yield **12** (106.6 mg, 62 %). Mp 232-233 °C. IR ν_{max} (HATR)/cm^{-1}: 3489 ν (OH), 1591, 1529 ν(NH-CO), 1683 ν(C=O), 1348, 1187 ν(SO_2). Found: C, 44.7; H, 3.4; $C_{15}H_{14}ClN_3O_6S$ $0.3H_2O$ requires C, 44.5; H, 3.6. m/z (EI, 70 eV) 399(M^+), 215(M^+-$C_8H_{10}NO_2S$), 188(M^+-$C_9H_9NO_3S$), 91(M^+-$C_8H_7ClN_3O_6S$).

Acknowledgements

This work was supported by CONACYT-México (832240-E). LHMH acknowledges financial support from CONACYT (Grant J-46308-Q). LM A-C thanks Alejandro Álvarez for reading the manuscript and for his helpful comments.

References

1. Lehn, J.-M. *Supramolecular Chemistry: Concepts and Perspectives;* VCH: Weinheim/New York, 1995.
2. Lehn, J.-M. *Angew. Chem. Int. Ed.* **1990**, *29*, 1304.
3. Pauling, L. *The nature of the chemical bond*. Cornell University Press: Ithaca, New York, 1939.
4. Desiraju, G. R. *Acc. Chem. Res.* **2002**, *35*, 565.
5. Reed, A. E.; Curtiss, L. A.; Weinhold, F. *Chem. Rev.* **1988**, *88*, 899.
6. Kolandaivel, P.; Nórmala, V. *J. Mol. Struct.* **2004**, *694*, 33.
7. Alabugin, I. V.; Manoharan, M., Peabody, S.; Weinhold, F. *J. Am. Chem. Soc.* **2003**, *125*, 5973.
8. Bent, H. A. *Chem. Rev.* **1961**, *61*, 275.
9. Rodríguez, A. D.; Ramírez, C.; Rodríguez, I. I.; González, E. *Org. Lett.* **1999**, *1*, 527.
10. Akahoshi, F.; Ashimori, A.; Sakashita, H.; Yoshimura, T.; Imada, T.; Nakajima, M.; Mitsutomi, N.; Kuwahara, S.; Ohtsuka, T.; Fukaya, C.; Miyazaki M.; Nakamura, N. *J. Med. Chem.* **2001**, *44*, 1286.
11. James, K. D.; Ekwuribe, N. N. *Synthesis* **2002**, 850.
12. Aguilar-Castro, L.; Tlahuextl, M.; Tapia-Benavides, A. R.; Tlahuext, H. *Heteroatom Chem.* **2003**, *14*, 247.
13. Tlahuextl, M.; Aguilar-Castro, L.; Camacho-Camacho, C.; Contreras, R.; Tapia-Benavides A. R. *Heteroatom Chem.* **2004**, *15*, 114.
14. Martínez-Martínez, F. J; Ariza-Castolo, A.; Tlahuext, H.; Tlahuextl, M.; Contreras, R. *J. Chem. Soc., Perkin Trans 2* **1993**, 1481.
15. Nakanishi, H.; Roberts, J. D. *Org. Magn. Reson.* **1981**, *15*, 7.
16. Binsch, G.; Lambert, J. B.; Roberts, B. W.; Roberts, J. D. *J. Am. Chem. Soc.* **1964**, *86*, 5564.
17. Gellman, S. H.; Adams, B. R.; Dado, G. P. *J. Am. Chem. Soc.* **1990**, *112*, 460.
18. Gellman, S. G.; Dado, G. P.; Liang, G.; Adams, B. R. *J. Am. Chem. Soc.* **1991**, *113*, 1164.
19. Dado, G. P.; Gellman, S. H. *J. Am. Chem. Soc.* **1993**, *115*, 4228.
20. Liang, G.; Desper, J. Gellman, S. H. *J. Am. Chem. Soc.* **1993**, *115*, 925.
21. Huheey, J. E. *Inorganic Chemistry*, 3rd Edn.; Harper International: Cambridge, USA, 1983; p 258.
22. Kupka, T.; Gerothanassis, I. P.; Demetropoulos, I. N. *J. Mol Struct.(Theochem)* **2000**, *531*, 143.
23. Meng, F.; Xu, W.; Liu Ch. *J. Mol. Struct. (Theochem),* **2004**, *677*, 85.
24. Avalos, M.; Babiano, R.; Barneto, J. L.; Bravo, J. L.; Cintas, P.; Jiménez, J. L.; Palacios, J. C. *J. Org. Chem.* **2001**, *66*, 7275.
25. Kang, Y. K. *J. Mol. Struct. (Theochem),* **2001**, *546*, 183.
26. Samdal, S.; Seip, R. *J. Mol. Struct,* **1997**, *413-414*, 423.
27. Becke, A. D. *J. Chem. Phys.* **1993**, *98*, 5648.

28. Becke, A. D. *Phys. Rev. A.* **1988**, *38*, 3098.
29. Lee, C.; Yang, W.; Parr, R. G. *Phys. Rev. B.* **1988**, *37*, 785.
30. Toyota, A.; Oki, M. *Bull. Chem. Soc. Jpn.* **1992**, *66*, 1832.
31. MOLEKEL 4.3, P. Flükiger, H. P.; Lüthi, S.; Portmann, J.; Weber, Swiss Center for Scientific Computing, Manno (Switzerland), 2000-2002.
32. Martínez-Martínez, F. J.; Padilla-Martínez, I. I.; Brito, M. A.; Geniz, E. D.; Rojas, R. C.; Saavedra, J. B. R.; Höpfl, H.; Tlahuextl, M.; Contreras, R. *J. Chem. Soc, Perkin Trans 2.* **1998**, 401.
33. Bruker Analytical X-Ray Systems. SAINT + NT, Version 6.01, 1999.
34. Bruker Analytical X-Ray Systems. SHELXTL-NT, Version 5.10, 1999.
35. Farrrugia, L. J. *J. Appl Cryst.* **1997**, *30*, 565.
36. Gaussian 98, Revision A.11, Frisch, M. J.; Trucks, G. W.; Schlegel, H. B.; Scuseria, G. E.; Robb, M. A.; Cheeseman, J. R.; Zakrzewski, V. G.; Montgomery, J. A.; Stratmann, R. E.; Burant, J. C.; Dapprich, S.; Millam, J. M.; Daniels, A. D.; Kudin, K. N.; Strain, M. C.; Farkas, O.; Tomasi, J.; Barone, V.; Cossi, M.; Cammi, R.; Mennucci, B.; Pomelli, C.; Adamo, C.; Clifford, S.; Ochterski, J.; Petersson, G. A.; Ayala, P. Y.; Cui, Q.; Morokuma, K.; Malick, D. K.; Rubuck, A. D.; Raghavachari, K.; Foresman, J. B.; Cioslowski, J.; Ortiz, J. V.; Stefanov, B. B.; Liu, G.; Liashenko, A.; Piskorz, P.; Komaromi, I.; Gomperts, R.; Martin, R. L.; Fox, D. J.; Keith, T.; Al-Laham, M. A.; Peng, C. Y.; Nanayakkara, A.; Gonzalez, C.; Challacombe, M.; Gill, P. M. W.; Johnson, B.; Chen, W.; Wong, M. W.; Andres, J. L.; Head-Gordon, M.; Replogle, E. S.; Pople, J. A. Gaussian, Inc., Pittsburgh PA, 1998.
37. Shao, Y.; Fusti-Molnar, L.; Jung, Y.; Kussmann, J.; Ochsenfeld, C.; Brown, S. T.; Gilbert, A. T. B.; Slipchenko, L. V.; Levchenko, S. V.; O'Neill, D. P.; DiStasio, Jr. R. A.; Lochan, R.C.; Wang, T.; Beran, G. J. O.; Besley, N. A.; Herbert, J. M.; Lin, C. Y.; Van Voorhis, T.; Chien, S. H.; Sodt, A.; Steele, R. P.; Rassolov, V. A.; Maslen, P. E.; Korambath, P. P.; Adamson, R. D.; Austin, B.; Baker, J.; Byrd, E. F. C.; Daschel, H.; Doerksen, R. J.; Dreuw, A.; Dunietz, B. D.; Dutoi, A. D.; Furlani, T. R.; Gwaltney, S. R.; Heyden, A.; Hirata, S.; Hus, C.; Kedziora, G.; Khalliulin, R. Z.; Klunzinger, P.; Lee, A. M.; Lee, M. S.; Liang, W.; Ritchie, J.; Rosta, E.; Sherrill, C. D.; Simmonett, A. C.; Subotnik, J. E.; Woodcock III, H. L.; Zhang, W.; Bell, A. T.; Chakraborty, A. K.; Chipman, D. M.; Keil, F. J.; Warshel, A.; Hehre, W. J.; Schaefer III, H. F.; Kong, J.; Krylov, A. I.; Gill, P. M. W.; Head-Gordon, M. *Phys. Chem. Chem. Phys.* In press.
38. GaussView, Version 3.0, Dennington II, R.; Todd, K.; Millam, J.; Eppinnett, K.; Hovell, W. L.; Gilliland, R. Semichem, Inc., Shawnee Mission, KS, 2003.
39. Glendening, E.D.; Reed, A. E.; Carpenter, J. E.; Weinhold, F. NBO (Version 3.1), Gaussian Inc, Pittsburg, PA, 2003.